Journal of Electronic Materials, Vol. 7, No. 2, 1978

STRUCTURAL STUDIES OF GRAPHITE INTERCALATION COMPOUNDS*†

D. D. L. Chung #

Department of Materials Science and Engineering

and Center for Materials Science and Engineering
Massachusetts Institute of Technology
Cambridge, MA 02139, USA

(Received July 14, 1977)

Electron diffraction through the c-face (layer planes) and scanning electron microscopy (SEM) on the a-face (perpendicular to the layer planes) have been used to study the intralayer crystal structure and the microstructure of graphite and its intercalation compounds. With the electron diffraction technique, the intralayer intercalate ordering and the associated order-disorder transformations have been studied in graphite-alkali metals (K, Rb, Cs) and graphite-halogens Br_2, IBr, ICl). Reported here is the first observation of

*Work supported by United States NSF Grant #DMR 76-12226.

†This paper is based on a thesis submitted by the author in partial fulfillment for the Ph.D. degree in the Department of Materials Science and Engineering, Massachusetts Institute of Technology, Cambridge, MA, USA, 1977 (unpublished).

#Present address: Department of Metallurgy and Materials Science and Department of Electrical Engineering, Carnegie-Mellon University, Schenley Park, Pittsburgh, PA 15213.

0361-5235/78/0300-0189$05.00/1

order-disorder transformations in the graphite-halogen compounds. Direct evidence is given for the presence of intralayer intercalate ordering in even extremely dilute lamellar and residue compounds. Also presented here is a new a-face surface preparation technique, which involves mechanical polishing and back-sputtering. SEM observations of the a-faces reveal large microstructural differences between highly-oriented pyrolytic graphite, chemically-separated single-crystal graphite and mechanically-separated single-crystal graphite. Significant exfoliation along the c-direction occurs upon intercalation. Evidence is given for the preferential trapping of intercalate at defects in both lamellar and residue compounds.

Key words: graphite, intercalation, intercalation compounds, graphite-halogens, graphite-alkali metals, structure.

Introduction

Graphite is one of the best examples of a layer material. Its intercalation compounds contain the foreign species (intercalate) in the interstitial layer planes of the graphite lattice, such that the layer structure of graphite is retained. Because of the potential as high electrical conductivity synthetic metals (1), graphite intercalation compounds have recently received considerable attention.

Graphite intercalation compounds can be classified into two groups: lamellar and residue compounds (2). Lamellar compounds exist in the presence of an equilibrium with the external intercalate. As soon as they are removed from this equilibrium (unless quenched to liquid nitrogen temperature or below), they desorb their intercalates. This desorption continues until the compound has come to equilibrium with a zero partial pressure of external intercalate, resulting in a residue compound. A residue compound usually contains about 1/3 of the intercalate of the parent lamellar compound. Because residue compounds are limited to relatively low intercalate concentrations, they have not received as much attention as the lamellar compounds. In this work, particular attention has been given to the comparison

between lamellar and residue compounds in terms of the intralayer intercalate ordering and the a-face microstructure.

The layer structure of graphite intercalation compounds presents unique features in both the crystal structure and the microstructure. The crystal structure (2) consists of an alternating sequence of intercalate monolayers separated by n contiguous graphite layers ($n \geq 1$), where n denotes the stage of the compound. The interlayer crystal structure varies with the intercalate concentration in the compound such that n increases with decreasing intercalate concentration. Moreover, the intercalate atoms or molecules within an intercalate layer are ordered at temperatures below the order-disorder transformation temperature for the intralayer structure of the particular intercalate (3). In this context, the crystal structure of graphite intercalation compounds involves two aspects, namely the interlayer ordering and the intralayer ordering. The interlayer ordering has been studied by many workers by means of x-ray diffraction (2). However, considerably less attention has been given to the studies of the intralayer ordering. The only compound of which the intralayer structure has been firmly established is the first stage graphite-K compound C_8K (4-6). Particularly for molecular intercalation compounds, such as graphite-Br_2 (7), graphite-ICl (8), graphite-$FeCl_3$ (9) and graphite-$MoCl_5$ (10), the intralayer structure is so complex that its complete determination is extremely difficult. This complexity is expected since the intercalate molecules can orient themselves at various angles with respect to the graphite lattice, in contrast to intercalate atoms which have essentially spherical symmetry. In the present work, attention is given to the effects of intercalate concentration and temperature on the intralayer structure of both lamellar and residue compounds.

Because of the layer structure, the microstructure of graphite intercalation compounds also involves two aspects: the microstructure on the c-face (the layer planes) and the microstructure on the a-face (the planes perpendicular to the layer planes and containing the c-axis). Due to the weak interlayer forces in graphite, the c-plane is the cleavage plane. Because of the nec-

essity for thin samples for transmission of the electron beam, the application of transmission electron microscopy to the study of the microstructure has been mostly limited to the situation in which the c-plane is the foil plane. Such studies have been carried out by a number of workers (11) and have revealed dislocations, stacking faults, Moiree patterns and other features. However much less is known concerning the microstructure on the a-face. Since graphite and its intercalation compounds are layer materials, the microstructure on the a-face should be very different and yet complementary to that on the c-face. Thus, attention has been given to the a-face in the present microstructural study by using scanning electron microscopy.

The intercalate ordering in graphite intercalation compounds is temperature-dependant, with order-disorder transformations due to interlayer ordering expected at a higher temperature T_u than the intralayer ordering temperature T_ℓ. At temperatures $T_\ell < T < T_u$ the carbon and intercalate layers are well ordered along the c-axis, but the intercalate is disordered within each intercalate layer. For $T > T_u$, the compound may become a disordered solid solution or become unstable thermodynamically. For $T < T_\ell$ 3-dimensional ordering is established. No order-disorder transformations have been reported for first stage graphite-alkali metal compounds. However, for the second stage graphite-alkali metal compounds, changes of observed x-ray diffraction patterns have been interpreted in terms of an intralayer order-disorder transformation (12, 13) in $C_{24}K$ at -175°C, $C_{24}Rb$ at -114°C and $C_{24}Cs$ at -110°C. Order-disorder transformations have also been studied in terms of anomalies in the temperature dependence of the transport parameters. Discontinuities in the temperature dependence of the electrical resistivity have been interpreted in terms of an order-disorder transformation at -20°C for graphite nitrate (14, 15). Preliminary results have also been reported on anomalies in the temperature dependence of the electrical resistivity of graphite-alkali metal compounds (16). In the present work, by observing the variation of the electron diffraction pattern with temperature, the order-disorder transformation associated with the intralayer intercalate ordering in graphite-halogens (Br_2, IBr, ICl) and graphite-alkali metals (K, Rb, Cs) have been investigated.

Of significance is that this work provides the first observation of the order-disorder transformation for the intralayer structure of the graphite-halogens.

There are two common types of graphite materials: pyrolytic graphite and single crystal graphite. Highly-oriented pyrolytic graphite (17) is synthetic and polycrystalline, with a texture such that the c-axis of all the crystallites are aligned to $\sim 0.2^o$ but the a-axis are random. The crystallite size is of the order of 1μ in both the a and c directions. On the other hand, single-crystal graphite is found in nature as flakes of 1 or 2 mm in diameter, embedded in calcite stones. To separate the flakes from the stone, chemical methods have usually been employed, by which the stone is immersed in boiling acids (HCl and HF) (18). Another separation method is mechanical by which mechanical shock causes the flakes to be separated from the stone. Most of the work done on graphite has been carried out with pyrolytic graphite or chemically-separated single-crystal graphite. In the present work, attention has been given to pyrolytic graphite and single-crystal graphite samples prepared by chemical and mechanical methods. Large differences in microstructure between the different graphite materials have been found. These differences have strong bearing on the electronic properties of these materials.

Experimental

Electron diffraction measurements through the c-face were made with a Philips EM300 transmission electron microscope using electrons of 80 or 100 kV and a diffraction area of a diameter of $\sim$ 1μ on the sample, which is based on highly-oriented pyrolytic graphite host materials (17). Because the in-plane crystallite size in this material is $\sim$ 1μ, the electron diffraction technique can provide information from a single crystallite. The electron beam is along the c-axis of the sample, so that the diffraction pattern obtained corresponds to the (001) reciprocal lattice plane. Therefore this technique is most sensitive to the intralayer ordering. For electron transmission, the specimen thickness has to be $\lesssim$ 1000Å. For each specimen, diffraction patterns were obtained at a number of different locations on the sample. The spec-

imens were prepared by cleavage from the bulk compound. For the graphite-alkali metals, which are air-sensitive, specimen preparation and mounting were carried out under nitrogen atmosphere in a glove bag. The specimens were quickly cooled to liquid nitrogen temperature after loading into the microscope in order to minimize intercalate desorption. The specimen temperature could be varied from liquid nitrogen temperature to $\sim$ 750°C by means of a cold stage and a hot stage equipped for the electron microscope.

Electron diffraction patterns have been obtained from lamellar and residue compounds of Br_2, ICl and IBr. Fig. 1 shows (001) electron diffraction patterns of pure graphite and several graphite-halogen compounds at room temperature.

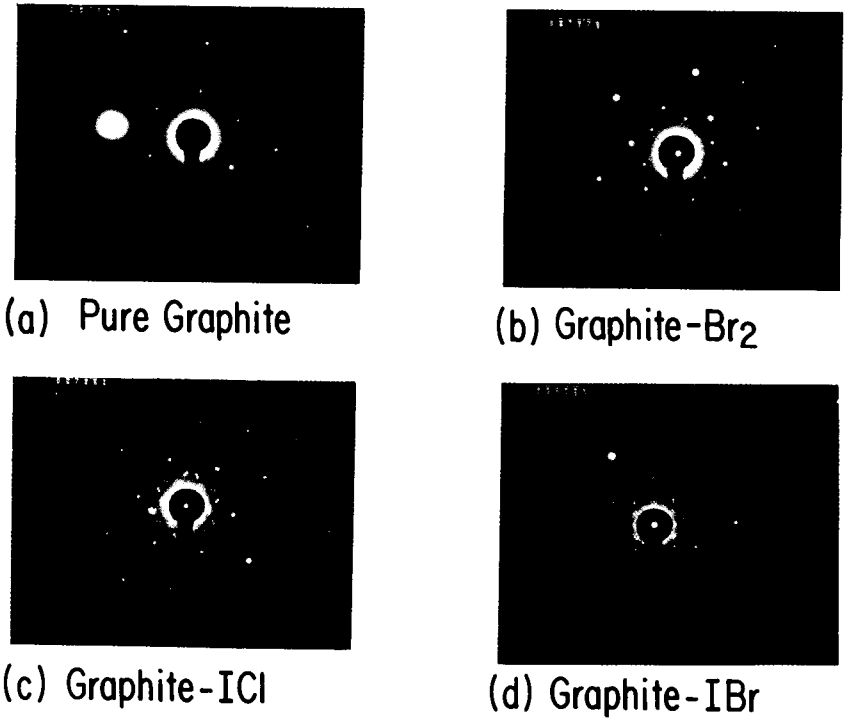

Fig. 1. Room temperature electron diffraction patterns of pure graphite and graphite-halogen compounds.

For each compound, in addition to the hexagonal pattern of diffraction spots due to graphite, there are superlattice diffraction spots. The superlattice diffraction patterns are different for different intercalates. The patterns for graphite-Br_2 and graphite-ICl have previously been reported by Eeles and Turnbull (7,8). The pattern for graphite-IBr is basically similar to that for graphite-ICl, but the relative distance between the various diffraction spots are different for the two interhalogens. The pattern for graphite-Br_2 is significantly different from those for graphite-ICl and graphite-IBr.

Investigation of the effect of intercalate concentration on the intralayer intercalate ordering has been carried out, with particular attention given to graphite-Br_2 lamellar and residue compounds, covering the entire range of intercalate concentration. Based on the electron diffraction patterns obtained for all the graphite-Br_2 compounds, it has been found that the intralayer intercalate ordering is relatively insensitive to the intercalate concentration, in contrast to the interlayer intercalate ordering (stage), which varies with the intercalate concentration. This means that an increase in intercalate concentration increases the number of intercalate layers without changing the arrangement of the intercalate within an intercalate layer.

Because the investigation of the crystal structure of graphite intercalation compounds has previously been carried out mostly on relatively concentrated lamellar compounds (2), information on the structure of dilute lamellar compounds and residue compounds has been limited. In fact, there has been considerable doubt in the presence of intercalate ordering in dilute compounds of stage $>> 5$, in addition to more concentrated lamellar compounds. This observation provides direct evidence for the presence of intralayer intercalate ordering in dilute lamellar compounds.

Because of the stability of residue compounds over that of lamellar compounds, residue compounds are more convenient to be used in practical applications. Therefore, the understanding of residue compounds is of importance. In this work, superlattice diffraction spots in the (001) electron diffraction patterns have been ob-

served in residue compounds of all intercalate concentrations - even as low as only 0.3 mole % Br_2. This observation shows that intralayer ordering is present in residue compounds, in support of the contention based on x-ray diffraction results (19). This observation further suggests that a significant portion of the intercalate in a residue compound resides in positions between the carbon layers, in contrast to the well-known concept that almost all of the intercalate in a residue compound resides at structural defects (20).

Significant changes in the electron diffraction patterns occur on raising the sample temperature above room temperature. For all the graphite-halogens, all the superlattice diffraction spots disappear when a critical sample temperature is reached. Above the critical temperature, which is different for different intercalates, the pattern is the same as that for pure graphite. This change, which is reversible on heating and cooling, is interpreted as an order-disorder transformation for the intralayer intercalate structure. Above the transformation temperature, the intercalate is disordered within each layer. The transformation temperature are 106°C, 60°C and 43°C for graphite-Br_2, graphite-IBr and graphite-ICl, respectively, with an error of ± 10°C. This is the first observation of order-disorder transformations for the intralayer intercalate structure in the graphite-halogens. These transformations have been observed in both lamellar and residue compounds.

Fig. 2 shows electron diffraction patterns of pure graphite and first stage graphite-alkali metal lamellar compounds at room temperature. The same electron diffraction pattern is found for the first stage graphite-K compound C_8K (Fig. 2b), and the first stage graphite-Cs compound C_8Cs (Fig. 2c), but differing from that observed in pure graphite (Fig. 2a). These first stage graphite-alkali metal electron diffraction patterns correspond to the reciprocal and real space in-plane unit cells shown in Fig. 3. This in-plane structure is consistent with x-ray diffraction results (4-6). The results reported here are contrary to those of Halpin and Jenkins (21), who attributed the pure graphite pattern shown in Fig. 2a to C_8K and attributed the pattern shown in Fig. 2b to a "heavily doped" graphite-K compound. These authors proposed that the intercalate layer stacking leads to the vanishing of all the superlattice diffraction spots in the (001) electron diffraction pattern. Order-disorder transformations have not been observed in C_8K or C_8Cs for temperatures up to ~ 200°C.

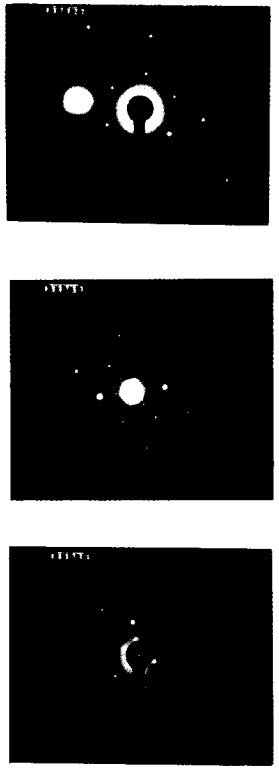

Fig. 2. Room temperature electron diffraction patterns of pure graphite and first stage graphite-alkali metal compounds.

The effect of intercalate desorption on the electron diffraction pattern of first stage graphite-Cs (C_8Cs) is shown in Fig. 4. Similar effects were observed for graphite-K and graphite-Rb. After slight desorption, a new pattern becomes superimposed on the stage 1 pattern (Fig. 4b). After more desorption the stage 1 pattern

is completely replaced by this new pattern (Fig. 4c).

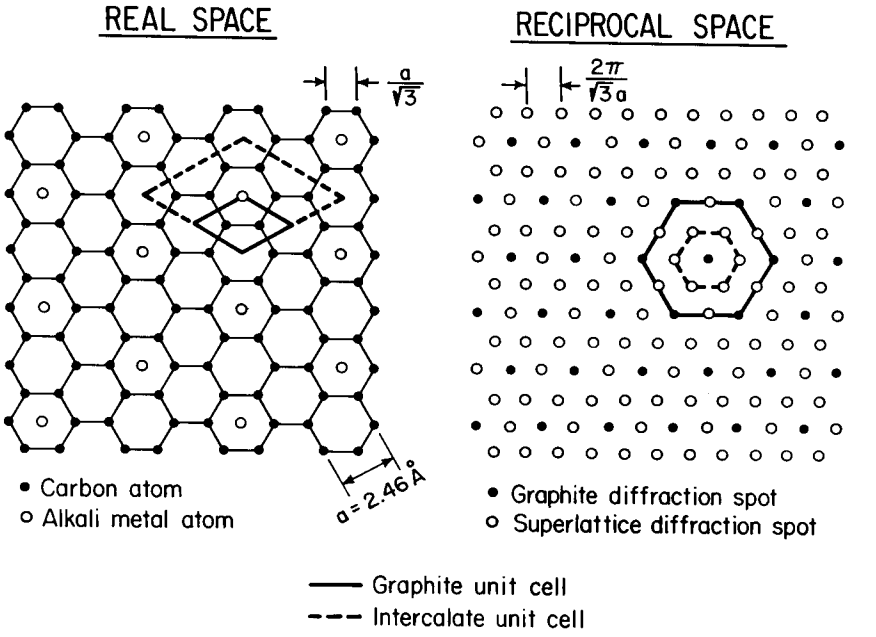

Fig. 3. Intralayer structure for first stage C_8X (X = K, Rb, Cs) in real space and reciprocal space.

Such patterns for the graphite-alkali metals (K, Rb, and Cs) are shown in Fig. 5, and this is the first reported observation of these electron diffraction patterns. The desorption was carried out for a few minutes or longer in a nitrogen atmosphere at room temperature, and resulted in greyish-blue compounds, typical of high stage graphite-alkali metals. The patterns in Fig. 5 are the most commonly observed patterns in this investigation and are interpreted to correspond to the intralayer structure of graphite-alkali metals of stage ≥ 2. The typical patterns for graphite-Rb and graphite-Cs are identical and are different from the typical pattern for graphite-K. However, on some portions of the graphite-K samples, the typical pattern for graphite-Rb (or graphite-Cs) was observed. A possible difference in the intralayer structure of graphite-K from that of graphite-Rb and graphite-Cs has also been reported by Parry et al. (13) based on x-ray diffraction intensity data.

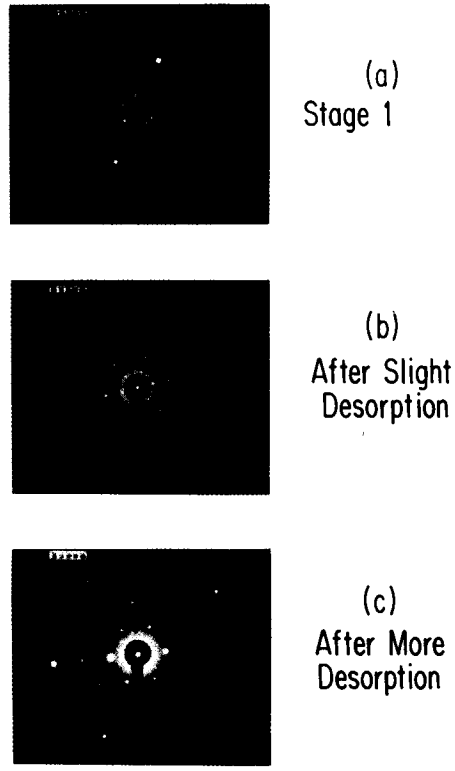

Fig. 4. Electron diffraction patterns of graphite-Cs on desorption from C_8Cs.

These patterns shown in Fig. 5 were obtained with the samples at liquid nitrogen temperature. As the sample temperature is raised, all the superlattice spots disappear, leaving a pure graphite pattern (Fig. 5a). This change is reversible on heating and cooling and is interpreted as due to an order-disorder transformation for the intralayer intercalate structure. The transformation temperatures are -63°C, -4°C and 5°C for graphite-K, graphite-Rb, graphite-Cs, respectively. Due to possible

specimen heating by the electron beam and the limitation in the accuracy of the measurement of the specimen temperature, these transformation temperatures are accurate to ± 15°C. These transformation temperatures are much higher than those previously reported for $C_{24}X$ (X = K, Rb, Cs) on the basis of x-ray diffraction studies (12, 13).

The electron diffraction patterns of Fig. 5 have been interpreted to yield real space unit cells, though the

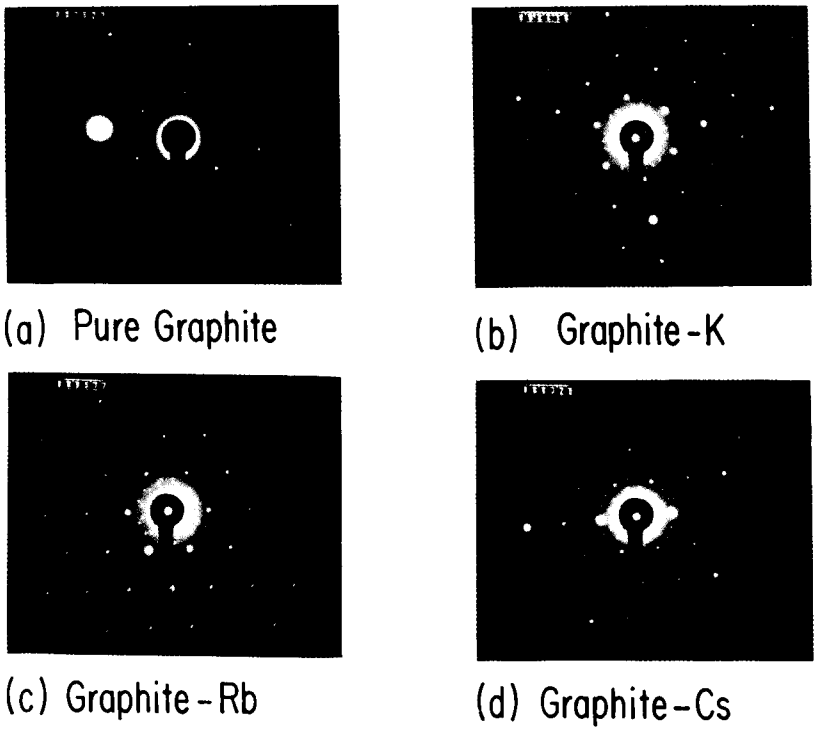

Fig. 5. Liquid nitrogen temperature electron diffraction patterns of graphite-alkali metal compounds after desorption from first stage has been completed.

arrangement of the alkali metal atoms within a unit cell has not yet been completely determined (3). Of significance is the observation that (i) the real space unit cell is very large for the three patterns shown in Fig.

5b, 5c, and 5d, (ii) these patterns are inconsistent with the simple unit cell proposed by Rüdorff and Schulze (5) for the higher stage graphite-alkali metal compounds. The reciprocal space structure corresponding to the unit cell proposed by Rüdorff and Schulze has not been observed either by x-ray or electron diffraction techniques. The x-ray diffraction data of Parry et al. (13) also do not support this commonly assumed in-plane structure.

To study the microstructure on the a-face, the author has used scanning electron microscopy (SEM). Because of the softness of graphite, a-faces are badly damaged and this surface damage must subsequently be removed. The author has therefore developed a technique for the pre-

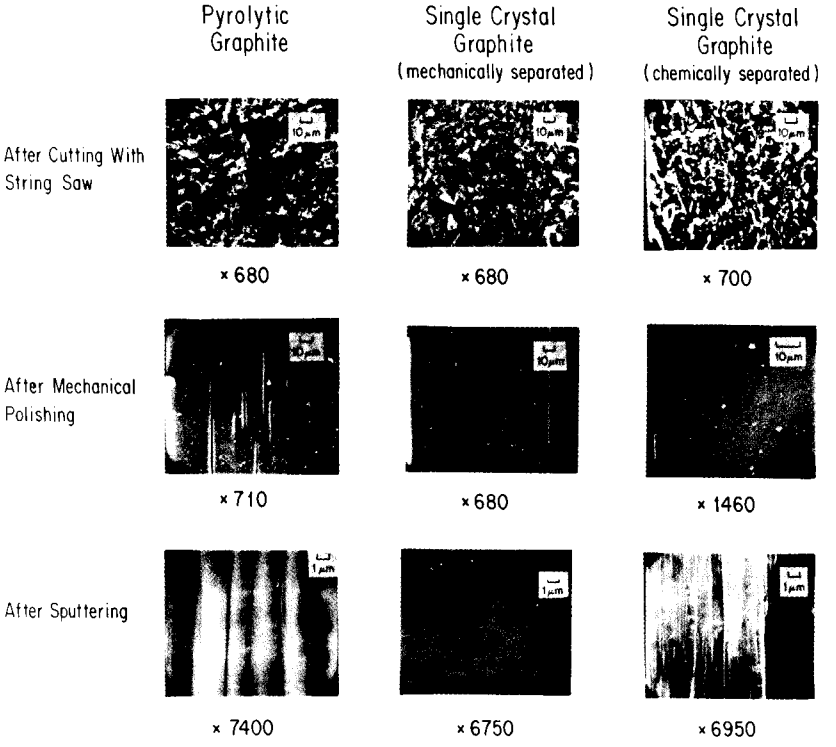

Fig. 6. Scanning electron microscope photographs of the a-faces of pure graphite.

paration of a-faces suitable for electron microscopy, optical reflectivity and light scattering studies. This technique involves mechanical polishing with alumina down to 0.06μ, followed by sputtering with argon at ∿ 10kV for a few hours. SEM photographs taken after each of these processes are shown in Fig. 6. Pyrolytic graphite and two kinds of single-crystal graphite were examined. One kind of single-crystal graphite was chemically separated from the ore-bearing calcite stone (18). The other kind of single-crystal graphite was mechanically separated from the stone. After cutting with the string saw, the a-faces of all the different kinds of graphite were badly damaged. After mechanical polishing, the a-faces were much smoother, but the surface damage was still present. After sputtering, numerous features were observed at high magnification. In pyrolytic graphite, thick dark lines, which are perpendicular to the a-axis, were observed with an average spacing of 2-3μ. These lines are interpreted as a combination of microcracks and boundaries of the crystallite layers. Between these lines, there are finer lines which are interpreted as clusters of dislocations or stacking faults intersecting the a-face. On the other hand, on the sputtered a-face of mechanically-separated single-crystal graphite, essentially no lines were observed. However, for the chemically-separated single-crystal graphite, there are many irregularly spaced lines. The difference between the mechanically-separated and chemically-separated single-crystal graphite indicates that the chemical separation intercalates or contaminates the single-crystal graphite. Since hydroflouric acid, which is used in the chemical separation, has been found to form intercalation compounds with graphite (22) it is suspected that the chemically-separated single-crystal graphite is not representative of pure graphite. Unfortunately, the single-crystal graphite materials which have been used for studies of the electronic properties by most workers were chemically separated.

Comparison between the sputtered a-faces of pyrolytic graphite and of mechanically-separated single-crystal graphite indicates that pyrolytic graphite has many microcracks and crystallite layer boundaries perpendicular to the c-axis, whereas mechanically-separated single-crystal graphite has negligible amounts of such defects. These structural defects should significantly decrease the c-

axis electrical conductivity and thus probably account for the large difference in the observed electrical conductivity anisotropy σ_a/σ_c between pyrolytic and single-crystal graphites (23).

The a-faces of the intercalation compounds examined on the SEM have been polished and sputtered prior to the

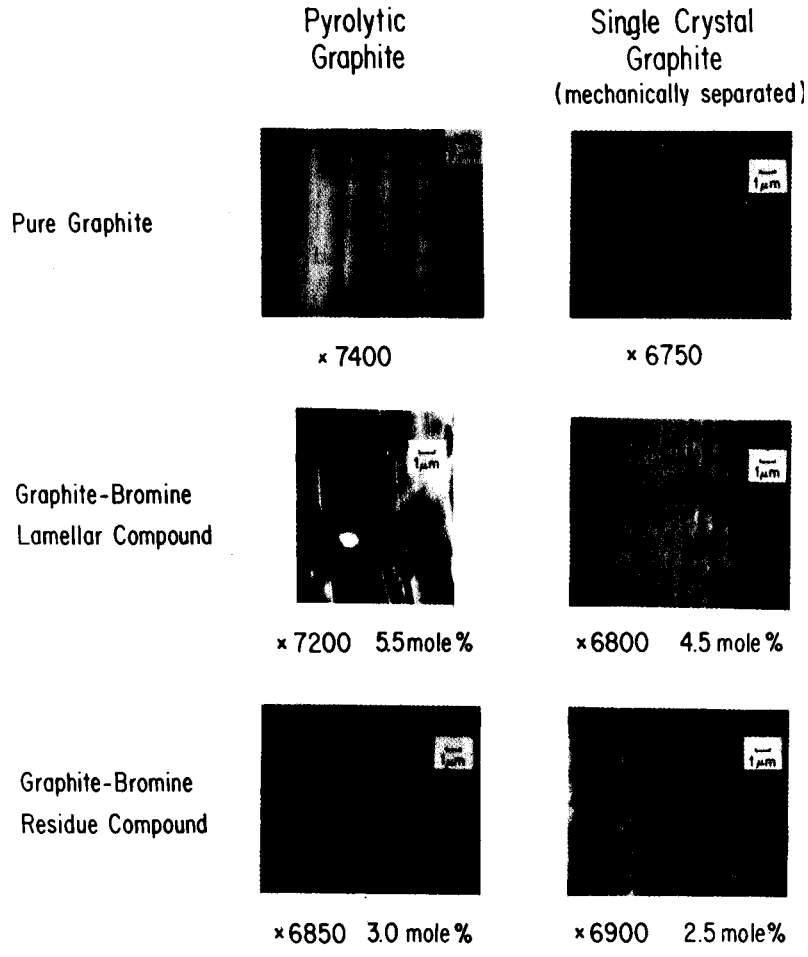

Fig. 7. Scanning electron microscope photographs of the a-faces of graphite-bromine lamellar and residue compounds.

intercalation process. The SEM observations were all performed on a Cambridge SEM with the specimens at room temperature. Thus this technique is restricted to desorbing lamellar compounds and to residue compounds.

Figure 7 shows SEM photographs of the a-faces of both lamellar and residue compounds of graphite-Br_2. The lamellar compound was prepared by exposure of the sputtered pure graphite to bromine vapor at room temperature and the residue compound was prepared by desorbing the parent lamellar compound in air at room temperature. The compositions of the compounds were determined by weight uptake measurements before and after the SEM observation. Because of the significant intercalate desorption which occurred in the lamellar compound, the intercalate concentration reported here for the lamellar compound is only a rough approximation. However, the intercalate concentration for the residue compound is accurate.

For the lamellar graphite-Br_2 compound based on pyrolytic graphite, the photograph in Fig. 7 shows that the crystallite layer thickness has increased from 2-3μ in pure pyrolytic graphite to 3-5μ in graphite-Br_2. Bromine intercalation can account for at most a 55% increase in the thickness. The rest of the observed increase is due to exfoliation. In addition, the finer lines between the crystallite layer boundaries are brighter and more pronounced than in the case of pure pyrolytic graphite. This effect observed upon intercalation is interpreted as due to the dislocations and stacking faults at which bromine tends to gather, thereby forming protrusions at the part of the surface where the dislocations and stacking faults intersect. That they are protrusions rather than depressions was established stereoscopically by means of parallax. In other words, SEM photographs were taken at different angles so that a three-dimensional image was produced when the photographs were viewed properly. In the residue compound, the various features on the a-face were less sharp than in the parent lamellar compound. Nevertheless, the SEM photograph shows that the crystallite layer thickness has decreased back to that of pure pyrolytic graphite.

For both the lamellar and the residue compounds based on mechanically-separated single-crystal graphite, the SEM

photographs show microcracks which were absent in the pure graphite. This observation provides further support for the fact that exfoliation along the c-direction is significant in both lamellar and residue compounds.

Graphite-ICl and graphite-IBr have also been investigated in a similar manner. Figure 8 shows a-faces of graphite-Br_2 (5.5 mole %), graphite-IBr (0.2 mole %) and graphite-ICl (8 mole %). All the compounds were prepared by exposing pure highly-oriented pyrolytic graphite to the respective intercalate vapor at room temperature. All of them exhibit the lines of protrusion associated with the intercalation process. In the graphite-ICl compound, the intercalate concentration is highest and the lines of

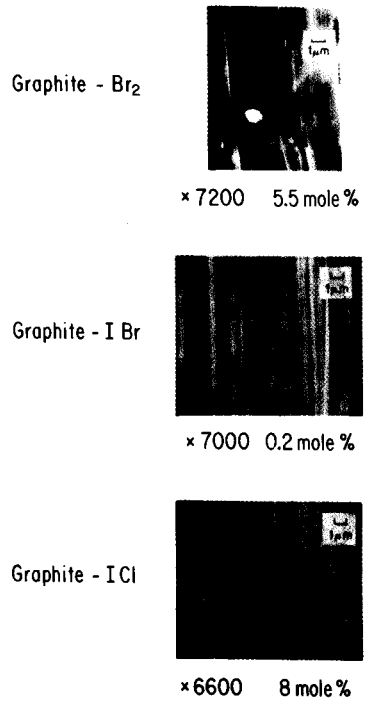

Fig. 8. Scanning electron microscope photographs of the a-faces of graphite-halogen lamellar compounds.

protrusion and microcracks are the densest.

Evidence in support of the preferential trapping of the intercalate at defect sites comes from scanning transmission electron microscope examination of the c-face of a graphite-Br_2 lamellar compound at room temperature.

Microscopic examination of the a-faces of lamellar and residue compounds of graphite-HNO_3 has also been carried out. The lamellar compound was prepared by exposure of pyrolytic graphite to the vapor of fuming nitric acid and the residue compound was obtained by desorption of the parent lamellar compound at room temperature in air above anhydrous Na_2CO_3. Both lamellar and residue compounds of graphite-HNO_3 show bright lines of thickness $\sim 1\mu$ and with an average spacing of $\sim 5\mu$. Between these thick lines, there are fine lines with an average spacing of $\sim 1\mu$. All these features were of a larger scale than those in the graphite-halogens. It thus appears that exfoliation is particularly severe in graphite-HNO_3. The large size of the acid molecule is probably responsible for this.

The author has also investigated the effect of pressure on exfoliation. It was found that applying pressure (~ 50 g/cm^2) on the c-face during Br_2 intercalation reduces the amount of exfoliation considerably. Thus for c-axis conductivity measurements, the samples should be prepared with the application of pressure in order to minimize exfoliation.

Discussion

The intralayer ordering has been given much attention in the present work by using electron diffraction through the c-face. In contrast to the interlayer ordering, which is relatively insensitive to the intercalate species, the intralayer ordering is different for different intercalate species. The complexity of the intralayer ordering is closely related to the size and symmetry of the intercalate species. Atomic or ionic intercalates, such as the alkali metals, have relatively simple intralayer structures, whereas molecular intercalates, such as the halogens, have complex intralayer structures and very large

in-plane unit cells. In addition to the size factor, the intralayer ordering for molecular intercalates is complicated by the orientations of the intercalate molecules relative to the graphite lattice.

Attention has also been given to the effect of intercalate concentration on the intralayer ordering. Detailed examination of graphite-bromine as a function of intercalate concentration indicates that the intralayer ordering is the same at all concentrations, ranging from 0.3 mole % Br_2 to near-saturation. This is consistent with Raman scattering (3, 24, 25) and infrared spectroscopy (3) observations, which show that the frequencies of the carbon atom in-plane vibrations do not change significantly with the intercalate concentration, which ranges from 0.2 mole % Br_2 to saturation in these experiments.

The intralayer order-disorder transformations in graphite-halogens and graphite-alkali metal compounds have been investigated by means of electron diffraction. The transformation temperatures are higher for graphite-halogens than for graphite-alkali metals of stage > 1. Among the graphite-alkali metals, the transformation temperature increases in the order K < Rb < Cs. This trend can be accounted for by consideration of the size of the alkali metal atom. The larger the atomic size, the more closely-packed is the intralayer structure and the harder it is for the atoms to move out of the ordered sites. This trend is consistent with the trend in the Raman structure in C_8X (X = K, Rb, Cs) at ~ 560 cm^{-1}, which indicates that the interaction between graphite and the intercalate is highest for Cs (25). Similar size considerations partly account for the higher transformation temperatures for the graphite-halogens than for the graphite-alkali metals. In addition to the size factor, the correlation of the various orientations of the halogen intercalate molecules may complicate the transformation mechanism for the graphite-halogens.

Particular attention has been given in this work to the comparison of residue compounds with lamellar compounds. The author has found that residue and lamellar compounds are similar in their intralayer intercalate ordering, although their interlayer ordering may be different. Thus the idea (20) that more than 99% of the

intercalate in residue compounds resides at defect sites is inconsistent with the electron diffraction results, which provide direct evidence for the presence of intercalate layers in residue compounds of all intercalate concentrations. Furthermore, based on electron microscopy on the a-face and on the c-face, this work provides evidence for preferential trapping of intercalate at defects in both lamellar and residue compounds. Therefore, the presence of intercalate at defects and on intercalate layers occurs in both lamellar and residue compounds though the fraction of intercalate at defects may be higher in residue compounds than in lamellar compounds. This conclusion is supported by the magnetoreflection results (3, 26), which indicate that the electronic band structures of dilute lamellar and residue graphite-halogen compounds of the same intercalate concentration ($\lesssim$ 1 mole %) are similar at energies within $\pm$ 0.1 eV from the graphite Fermi energy, but the relaxation time τ is longer in lamellar compounds than in residue compounds of the same intercalate concentration. Further support is provided by the Raman (3, 24, 25) and infrared (3) results, which indicate that the graphitic and intercalate vibrations are similar in lamellar and residue compounds, though the intensities of the lines are slightly different for lamellar and residue compounds of the same intercalate concentration.

Addendum

Neutron scattering data have recently indicated an intralayer order-disorder transformation at 474°C in the first stage graphite-Rb compound C_8Rb (27). An anomaly in the temperature dependence of the a-axis electrical conductivity has recently been found at 37°C in graphite-ICl (28), in agreement with the order-disorder transformation first observed by the author at 43 $\pm$ 10°C by means of electron diffraction.

Acknowledgements

The author would like to thank Prof. J. Vander Sande and Prof. M. S. Dresselhaus for helpful discussions.

References

1. A. R. Ubbelohde, Carbon 14, 1 (1976).
2. W. Rüdorff, Adv. Inorg. Chem. 1, 223 (1959).
3. D. D. L. Chung, Ph.D. thesis, Department of Materials Science and Engineering, Massachusetts Institute of Technology, Cambridge, MA 02139, USA (1977).
4. A. Schleede and M. Wellmann, Z. Phys. Chem. B18, 1, (1932).
5. W. Rüdorff and E. Schulze, Z, Anorg. allgem. Chem 277, 156 (1954).
6. D. E. Nixon and G. S. Parry, Brit. J. Appl. Phys. 1, 291 (1968).
7. W. R. Eeles and J. A. Turnbull, Proc. Roy. Soc. (London) A283, 179 (1965).
8. J. A. Turnbull and W. T. Eeles, 2nd Conf. Ind. Carbon and Graphite, 1965, Soc. Chem, Ind. London, p. 173 (1966).
9. J. M. Cowley and J. A. Ibers, Acta Cryst. 9, 421 (1956).
10. A. W. Symme Johnson, Acta Cryst. 23, 770 (1967).
11. M. Heerschap, P. Delavignette and S. Amelinckx, Carbon 1, 235 (1964).
12. G. S. Parry and D. E. Nixon, Nature 216, 909 (1967).
13. G. S. Parry, D. E. Nixon, K. M. Lester and B. C. Levene, J. Phys. C. 2, 2156 (1969).
14. D. E. Nixon, G. S. Parry and A. R. Ubbelohde, Proc. Roy. Soc. London Ser. A291, 324 (1966).
15. A. R. Ubbelohde, Proc. Roy Soc. A304, 25 (1968).
16. D. G. Onn, G. M. T. Foley and J. E. Fischer, Bull Am. Phys. Soc. 22, 421 (1977).

17. A. W. Moore, Chemistry and Physics of Carbon 11, 69 (ed. P. L. Walker) Dekker, New York, (1973).

18. W. P. Eatherly, private communications (1975).

19. J. Maire and J. Mering, Proc. of 3rd Carbon Conf., Buffalo, 1957. Pergamon Press, New York, p. 337 (1959).

20. G. R. Hennig, J. Chem. Phys. 20, 1438 (1952).

21. M. K. Halpin and G. M. Jenkins, 3rd Conf. on Ind. Carbons and Graphite, Soc. Chem. Ind., London, p. 53 (1970).

22. A. A. Opalovaskii, A. S. Nazarov, A. A. Uminskii and Yu. V. Chicagov, J. Inorg. Chem. 17, 1227 (1972).

23. I. L. Spain, Chemistry and Physics of Carbons 8, 1 (ed. Walker and Thrower), Dekker, New York (1973).

24. J. J. Song, D. D. L. Chung, P. C. Eklund and M. S. Dresselhaus, Solid State Comm. 20, 1111 (1976).

25. P. C. Eklund, G. Dresselhaus, M. S. Dresselhaus and J. E. Fischer (to be published).

26. D. D. L. Chung and M. S. Dresselhaus, Physica 89B, 131 (1977).

27. W. D. Ellenson, D. Semmingson and J. E. Fischer, Proceedings of the International Conference on Intercalation Compounds of Graphite, to be published in J. Mat. Sci. Eng., December 1977.

28. D. G. Onn et al., to be published.